

Hydrogen Cycle on CeO₂ (111) Surfaces: Density Functional Theory Calculations

Matthew B. Watkins,^{*,†} Adam S. Foster,[‡] and Alexander L. Shluger[†]

Department of Physics and Astronomy, University College London, Gower Street, London WC1E 6BT, U.K., and Laboratory of Physics, Helsinki University of Technology, P.O. Box 1100, Helsinki 02015, Finland

Received: March 2, 2007; In Final Form: July 1, 2007

We studied the interaction of perfect and lightly reduced ceria (111) surfaces with hydrogen and water molecules using density functional calculations implementing the generalized gradient approximation (GGA) and on-site Coulomb interactions (GGA+U). We predicted the relative surface energies at different states of reduction and in the presence of water, allowing insight into surface processes under a variety of conditions. Several unusual properties of the ceria surface were brought to the fore: the dissociation of water molecules on the ideal surface, the rapid dissociation of water at vacancy sites, and the strongly exothermic dissociation of H₂ on the ideal surface. These results have strong implications for the interpretation of experimental data and the construction of reaction schemes for this technologically important metal oxide surface.

Introduction

Ceria is an important surface for many applications, particularly catalysis. Its ability to accommodate varying charge states facilitates relatively facile surface oxidation/reduction that allows it to mediate the oxygen concentration when it is part of a mixed metal oxide catalyst.^{1–4} There is an extensive literature on the reduction/oxidation behavior; however, experimental conditions and uncertainties in sample preparation complicate interpretation of experimental data. It is now appreciated that the extent of hydroxylation of metal oxide surfaces can have a significant effect on their properties, especially those that are highly surface dependent. Water is virtually impossible to exclude from realistic environments, and its behavior on a variety of metal oxide surfaces, particularly TiO₂, has been extensively studied.^{5–7} Often, the interplay between associated/dissociated states and interactions with surface defects are complex and connecting theoretical calculations to experiment can be difficult.^{8–10} Another aspect of the redox behavior of ceria is its reduction under a H₂ atmosphere. Generally, there appear to be two peaks in the temperature-dependent reduction measurements: one at around 770 K and another at 1100 K.^{1–4} The high-temperature peak is interpreted as arising from bulk reduction, whereas the lower temperature peak at 770 K, which is not observed in samples with low surface area, is interpreted as arising from the reduction at surfaces.

In this article, we present the results of *ab initio* calculations that shed light on the thermodynamics of surface reduction and the probable state of lightly reduced surfaces in the presence of water, allowing insight into surface processes under a variety of conditions.

Computational Details

We considered two types of surfaces: fully oxidized CeO₂ (111) and reduced CeO₂ (111) where a single oxygen vacancy was introduced into the simulation cell. Both of these systems

have been examined theoretically in the past few years.^{11–13} However, the electronic structure of the reduced ceria surface is still somewhat controversial. Reduction of the surface, by either oxygen vacancy formation or hydrogenation, produces extra electrons that must occupy either conduction-band states or states localized within the band gap. Depending on the character of the metal(s) present, these electrons are accommodated in two qualitatively different ways in metal oxides: either the electrons are located predominantly in a vacancy site, e.g., F center in MgO, or, if the metal is easily reduced, extra electrons reside on metal ions and a mixed-valence compound is formed, e.g., TiO₂. Ceria is readily reduced, because of the presence of the low-lying 4f states; however, a further question is whether *individual* Ce⁴⁺ ions are reduced to Ce³⁺ ions or whether electrons are delocalized over many metal atoms. To cover both possibilities, the plane-wave density functional theory (DFT) calculations in this work were carried out using two related functionals: one using the generalized-gradient approximation (GGA) and another incorporating a local on-site Coulomb repulsion term (GGA+U) within the formulation of Dudarev et al.¹⁴ as implemented in the VASP package.¹⁵ More specifically, we used PW91-GGA^{16–18} and PW91-GGA+U functionals, which are expected to cover the two extremes: GGA usually causes excess electrons to be delocalized over several Ce ions, whereas GGA+U is designed to localize one electron per Ce³⁺ ion. As described in refs 14 and 19, in the latter case, a Hubbard-U term is added to the plain GGA functional. This additional exchange repulsion term serves to stabilize solutions to the Kohn–Sham problem with localized electrons on cerium. As a further check on our results, we repeated the majority of the calculations with the local density approximation (LDA) to ensure that the results were not unduly sensitive to the exact form of the exchange-correlation functional used, though without the addition of the Hubbard-U correction.

The value of $U = 5$ eV used in our calculations should be considered as an empirical parameter. It was optimized to position the cerium 4f states at ~ 1.3 eV above the oxygen 2p states in bulk Ce₂O₃, as determined from the onset of PES signals attributed to Ce³⁺ 4f electrons²⁰ (3.6 eV was obtained

* To whom correspondence should be addressed. E-mail: matthew.watkins@ucl.ac.uk.

[†] University College London.

[‡] Helsinki University of Technology

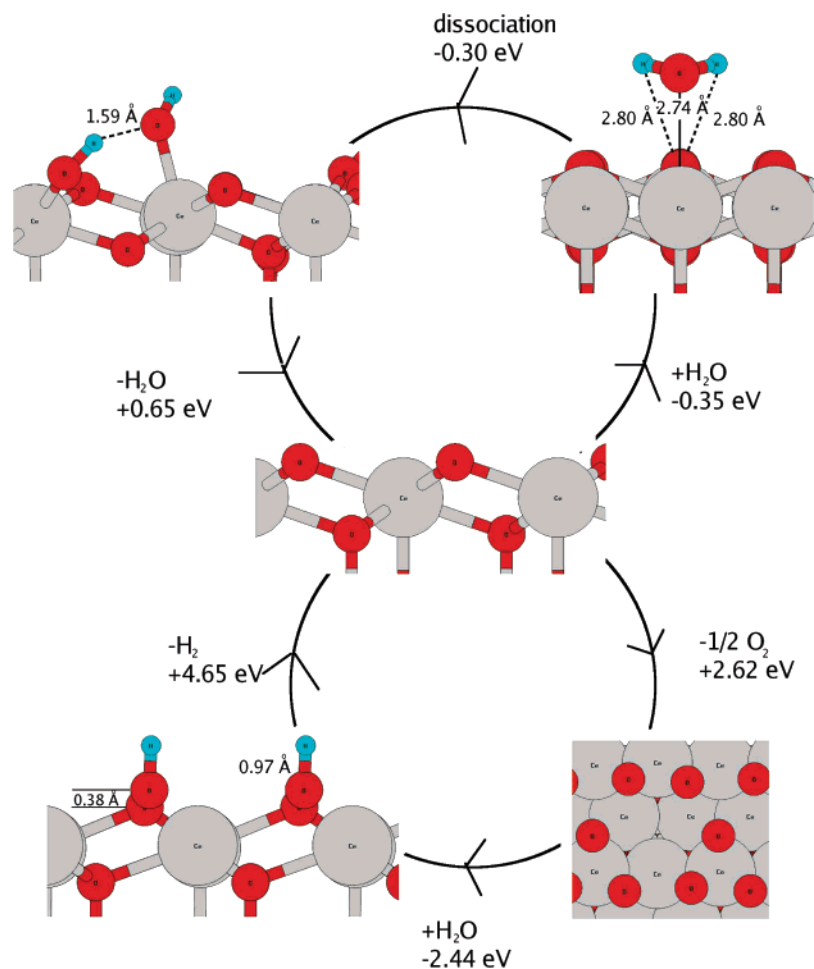


Figure 1. Reactions of water on the reduced and ideal ceria (111) surfaces. Important bond lengths are marked; energetics are from the GGA+U calculations (see Computational Details). The large chemisorption energy of H_2 (4.65 eV) is the reverse of the energy of adsorption of H_2O at a vacancy.

with the GGA functional). We should note, however, that direct comparison between the merits of the two pictures is difficult and the implementation of GGA+U used here has certain problems.²¹ Within a plane-wave implementation of DFT, the inclusion of the Hubbard-U term requires that the wavefunction be projected onto a local atomic basis, in this case, a set of spherical harmonics within some assumed Wigner–Seitz radius centered on the atoms (1.323 and 0.82 Å for cerium and oxygen, respectively). However, this projection, especially if there is some degree of covalency, is somewhat arbitrary, and even in pure ceria, some fractional occupancy of the cerium 4f states (mixed into the valence band) will be found, which is energetically penalized by the functional. Ce^{3+} has a larger atomic radius than Ce^{4+} , and consequently, bond lengths around a Ce^{3+} ion will be increased; this reduces the spurious penalty due to the fact that the projection scheme unphysically stabilizes the reduced state. This is also the origin of the increase in calculated lattice constant for CeO_2 within GGA+U compared to GGA (5.49 vs 5.43 Å; the appropriate theoretical bulk lattice constant was always used in our calculations). The LDA functional, as expected, predicts a smaller lattice constant of 5.36 Å. In all calculations, the equilibrium lattice constant for the appropriate density functional was used.

Periodic boundary conditions were used throughout the calculations. A plane-wave cutoff of 500 eV converged the total energy to 4 meV per CeO_2 unit in bulk ceria and was used with projector augmented-wave (PAW) pseudopotentials.²² A

$3 \times 3 \times 1$ Monkhorst–Pack k -point grid was used for $2 \times \sqrt{2}$ surface cells, and Γ point was used only for the larger cells. In surface calculations, we used periodic slabs that were nine atomic layers thick and were separated by a 15-Å vacuum gap. This slab thickness was found to be sufficient to converge the surface energy to 0.01 J/m². All calculations were performed using spin-polarized functionals, which were essential for all systems where the ceria surface was reduced, and structures were considered to be relaxed when ionic forces were less than 0.03 eV/Å. All energies quoted are for the GGA+U functional (GGA in parentheses) unless otherwise stated. To test some of our predictions and to gain more insight into the dynamics of adsorption and dissociation processes, we also ran molecular dynamics (MD) calculations using an *NVE* microcanonical ensemble. These MD simulations were started from fully relaxed geometries, the plane-wave energy cutoff was reduced to 350 eV, and the final temperature was approximately 300 K.

Given that both the water molecule and any dissociation products formed have a significant dipole, it was important to check that our results were converged with respect to the supercell size. To check this, we calculated the energies of adsorption, dissociation, and separation of dissociated products on the ideal surface using the GGA+U functional for three supercell sizes: $2 \times \sqrt{2}$, $4 \times \sqrt{2}$, and $4 \times 2\sqrt{2}$. The results show that the energies calculated differ by no more than 0.12 eV between the different cells. The results show a linear relation plotted against R^{-3} , where R is the average distance between

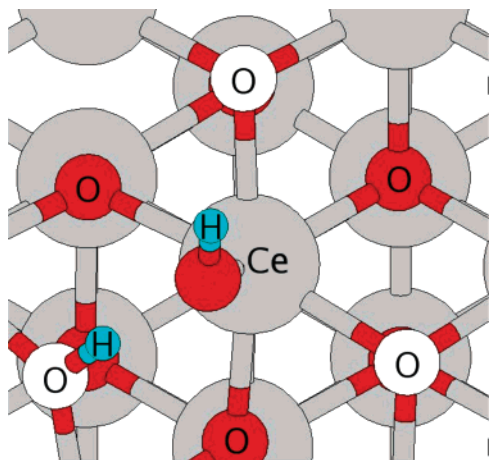


Figure 2. Dissociated water molecule having three equivalent binding sites (white oxygen ions) with a proton from water transferring to either of the three highlighted surface O atoms neighboring the cerium adsorption site of the water molecule. A top view of the relaxed geometry of a single configuration is shown.

images of defects in the supercells considered, as expected for artificial dipole or elastic interactions due to finite supercell size. Given the magnitude of the energies we were considering, we were happy with this level of convergence with cell size and considered the reduced surface only using the smaller cell. The interaction of periodically repeating images in the z direction (perpendicular to the slab) was found to be negligible, on the order of 1 meV, obtained by introducing a dipole layer into the vacuum region to decouple the artificial interaction introduced by the boundary conditions.

Using these methods, we obtained good agreement with the previous calculations carried out with similar techniques, particularly quantitative agreement with the calculations of Nolan et al. for the CeO₂ (111) surface energy and vacancy formation energy.¹³ As has been discussed previously,^{13,19} the electrons remaining in the surface on vacancy formation are localized on 4f orbitals of Ce ions neighboring the vacancy site when the Hubbard-U term is included in the functional or delocalized across the top layer of cerium ions using the GGA functional.

Results

First, we considered H₂O adsorbing on the ideal surface. The adsorption energy was found to be -0.36 (-0.35) eV and corresponds to a state with the water bound to a Ce ion by the oxygen with the two hydrogens oriented toward a single oxygen of the ceria surface (upper right of Figure 1). Because of the symmetry of the ceria surface, there are three equivalent configurations for this physisorbed water molecule (Figure 2 shows the equivalent top-layer oxygen atoms). A further energy gain of -0.3 eV occurs if the water molecule dissociates, leaving an OH group bound to the initial physisorption site and another OH group formed by transfer of a proton from water to a surface O ion; we note that there are three equivalent surface sites (Figure 2). The energy to separate the two OH groups to next-nearest sites is $+0.5$ eV. The surface O–H bond distance is also longer than a typical O–H bond at 1.03 Å. To determine whether there was a significant barrier to dissociation, a molecular dynamics simulation was run, and dissociation of the H₂O molecule was observed within 50 fs, which suggests that dissociation will be facile at room temperature. The distance between the two O ions forming OH bonds is only 2.52 Å,

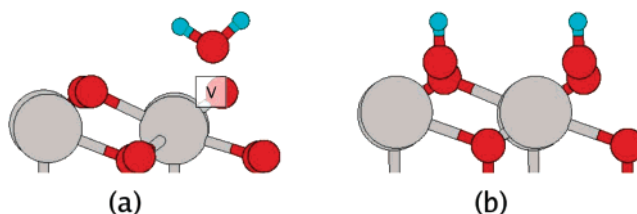


Figure 3. H₂O adsorption at a vacancy site on CeO₂ (111): (a) physisorbed H₂O at a vacancy and (b) H₂O dissociated to form two surface OH groups.

which can be expected to fall into the range of “strong” hydrogen bonds²³ where the potential energy surface for the motion of the proton between the two O ions has a single broad, strongly asymmetric minimum. In this case, the proton lies closer to the surface O, implying that the ceria surface is more basic than water.

The interaction of H₂O with the reduced surface is much more dramatic. The water molecule binds to the vacancy site with an energy gain of -0.8 eV (Figure 3a). Upon dissociation (Figure 3b), a further gain of -1.7 eV occurs, giving a total reaction energy of -2.45 (-2.45) eV. Two surface OH groups are formed with the water oxygen occupying the original vacancy site. To check whether the dissociation could occur readily, another molecular dynamics simulation was carried out. H₂O dissociation was found to occur within 100 fs. As noted above, two cerium ions neighboring the vacancy are reduced to Ce³⁺ when the on-site Coulomb correction term is included. The localization of these electrons is not strongly influenced by the presence of water, as the energies of the localized states shift by less than 0.2 eV. The dissociated water molecule then forms two charge pairs: two OH groups with a positive charge compared to an ideal lattice oxygen site and two Ce³⁺ ions with a negative relative charge. Separation of the two charge pairs into isolated groups was calculated to be energetically neutral and, hence, will be controlled by the kinetics of their motion. We emphasize that this means that observation of, e.g., XPS signals attributed to Ce³⁺²⁴ does not necessarily imply the existence of vacancies. Although hydroxyl groups and vacancies might not be distinguishable via XPS or magnetic balance measurements, they could exhibit quite different chemistry on the surface, acting as trapping centers for different species. A possible means of discriminating between OH groups and vacancies would be to correlate XPS signals with OH bond IR signals.²⁵

As shown in Figure 1, calculations of water at a vacancy site allowed us to obtain the energy of H₂ dissociation into two OH groups at the ideal surface with two electrons transferring to Ce ions. We found that the dissociation of H₂ on the terrace of CeO₂ (111) is strongly exothermic at -4.65 (-3.24) eV per molecule of H₂. The GGA and LDA results of -3.24 and -3.37 eV, respectively, although smaller than the GGA+U value, confirm that the H₂ dissociation is a strongly exothermic process. The smaller energy for GGA is expected,²¹ as the GGA+U functional tends to overestimate the stability of the reduced ceria surface (see discussion below).

The large energy gain upon hydrogen dissociation can be attributed to the unusual properties of the cerium 4f states. Instead of the two electrons originally forming the H–H bond having to be located in the conduction band formed by cerium 5d orbitals at ca. 6 eV above the valence band, the 4f states provide levels at approximately 1.5–2.5 eV above the valence-band maxima. This is a reflection/cause of the large electron affinity of Ce⁴⁺ and drives this reaction. We note that after, the

TABLE 1: Comparison of Reaction Energies with Different Functionals

reaction	reaction energy (eV)		
	LDA	GGA	GGA+U
water physisorption on ideal surface	-0.60	-0.32	-0.35
water dissociation on ideal surface	-0.79		-0.53
hydrogen-atom chemisorption energy		-4.09	-4.61
oxygen vacancy formation energy	+4.08	+3.76	+2.63
physisorption of H ₂ O at vacancy site	-1.01		-0.79
chemisorption of H ₂ O at vacancy site	-2.42	-2.17	-2.45

initial reaction, two main channels for further reaction are available: the two OH–Ce³⁺ centers can diffuse apart, or H₂O can be released from the surface in the reverse of the reaction considered in the previous paragraph, forming a vacancy site at the surface. These processes would form one or two electron defect sites on the ceria surface, respectively.

Discussion and Conclusions

Several of the results above demonstrate the rather unusual properties of ceria and, as such, need to be placed into a wider context. First, we comment on how the methods of calculation, specifically the functionals used, might influence the results. Table 1 provides a comparison of the three functionals used for each reaction considered. Energies for reactions with similar numbers of Ce³⁺ ions appear little affected by the choice of functional, e.g., the water adsorption energy is -0.325 eV with GGA+U and -0.353 with GGA, and the dissociation energy of H₂O at a vacancy is -2.45 eV with GGA+U and -2.17 eV with the GGA functional. However, when excess electrons have been transferred to the surface, there is a sizable difference in the energetics between the two functionals. This error appears to be largely systematic: the difference in energy between the two functionals for the one-excess-electron system [Ce³⁺–OH] is 0.52 eV, whereas for the two-electron centers considered, it is 1.14 and 1.41 eV (for the vacancy and 2[Ce³⁺–OH] systems, respectively). Fabris et al.²¹ found a shift of 1.4 eV for the two-electron reduction process CeO₂ → 1/2Ce₂O₃ + 1/2O₂. We also note that the reduction energy for the process CeO₂ → 1/2Ce₂O₃ + 1/2O₂ is overestimated in the GGA approach by ~0.35 eV.²¹ In the cases considered, there are no significant differences between the LDA and GGA functionals.

Our calculations demonstrate that the dissociation of water at the ideal surface of ceria (111) is promoted by the formation of a strong hydrogen bond between the OH⁻ and H⁺ moieties created. During the equilibration period of our MD simulations of H₂O adsorption at the ceria surface, we also observed a diffusion event where the H₂O molecule almost desorbed from the surface; a small interaction with the surface remained, and the water molecule reoriented itself during its motion to keep a proton pointing to a surface O ion. This is a possible mechanism of diffusion of a H₂O molecule on the ceria surface by molecular desorption and movement to an adjacent site, although motion of the OH groups while dissociated could also contribute to surface mobility. There are three equivalent dissociated, but closely bound states for the water molecule (Figure 2), and they are expected to be dynamically occupied at room temperature. The frequency of such diffusion can be roughly estimated by taking the rate equation to be of the form of an attempt frequency multiplied by a Boltzmann factor. Our calculations allowed us to estimate an upper limit to the energy barrier for reorientation as the difference in energy of the molecularly adsorbed water molecule and the dissociated state, as observed in our MD run. Using a typical phonon frequency of 10¹³ Hz and our barrier of ~0.3 eV to re-form the molecular physisorbed water species,

the rate of motion between the three equivalent dissociated states would be ~3.1 MHz. Thus, any noninvasive probe observing on a time scale of microseconds or longer would see only an averaged configuration.

The large energy for water dissociation at vacancy sites has a precedent in calculations on TiO₂. For titania, calculations suggest that the dissociation is exothermic by -1.35 eV on anatase surface vacancies.²⁶ In the titania structure, the missing O site is only two-coordinate and has a lower Madelung potential than the vacancy on ceria (111) where the site has three cerium neighbors. A recent work²⁷ appears to contradict this result, finding that the dissociation of water at oxygen vacancies is unfavorable. However, the investigation in ref 27 actually models a quite different situation. A supercell one-half the size of our smallest model was used, and as a consequence, the model system had an infinite chain of oxygen vacancies. A calculation using the smaller supercell for a surface oxygen vacancy confirmed their result: In the infinite chain, there was a strong collective relaxation of a second-layer oxygen toward the vacancy site; the presence of this raised oxygen atom then blocked the dissociation of water in the short MD run they performed. This upward relaxation of second-layer oxygen atoms could be of some significance for the extended defects observed by STM.¹¹ These systems are in contrast to, e.g., MgO, where the metal is not reducible and electrons in the vacancy site prevent the dissociation of water from being so favorable (although molecular dynamics simulations in ref 28 suggest that dissociation can still occur). The predicted rapid dissociation of H₂O at vacancy sites appears to be at odds with the experimental observation of reversible water adsorption on heavily reduced ceria samples.²⁴ We suggest, however, that the energies we found are beyond the likely error of the calculation methods used (particularly given the agreement between the density functionals) and that the heavily reduced sample used by Henderson et al.²⁴ (estimated 44% surface reduction) had reconstructed to areas of Ce₂O₃ through the aggregation of mobile vacancies at the elevated reduction temperatures used.

To summarize, these results show that water dissociation at vacancy sites is expected to be rapid, but notably, will not change the character of electrons originally localized on cerium ions neighboring the vacancy. We also predict a strongly exothermic character for H₂ chemisorption on the ideal ceria (111) surface, which we attribute to the low-lying 4f states, and hence large electron affinity, of ceria. The dissociated water molecule forms two charge pairs: two OH groups with a positive charge compared to an ideal lattice oxygen site and two Ce³⁺ ions that would not be differentiated from vacancy sites using XPS or similar experimental techniques. Finally, we have shown that the dissociation of water is favored on the ideal surface of ceria (111) and suggest that this is due to fortuitous lattice spacing allowing the formation of a strong hydrogen bond between the OH⁻ and H⁺ moieties formed upon dissociation. This would allow dynamic reorientation of H₂O on a megahertz time scale and a low diffusion rate on the order of seconds.

Acknowledgment. M.B.W. acknowledges financial support from EU FP6 Project “Nanoman”. We are grateful to S. Grischneider, M. Reichling, F. Esch, S. Fabris, P. Lindan, A. Sokol, and G. Thornton for valuable and encouraging discussions. Computer resources on CSAR and HPCxx were provided via our membership in the U.K.’s HPC Materials Chemistry Consortium and funded by EPSRC (Portfolio Grant EP/D504872). ASF is grateful to the Centre for Scientific Computing, Espoo, Finland, for computing resources.

References and Notes

- (1) Bernal, S.; Calvino, J. J.; Cifredo, G. A.; Rodriguezquintero, J. M.; Perrichon, V.; Laachir, A. Reversibility of Hydrogen Chemisorption on ac Ceria-Supported Rhodium Catalyst. *J. Catal.* **1992**, *137* (1), 1–11.
- (2) Laachir, A.; Perrichon, V.; Badri, A.; Lamotte, J.; Catherine, E.; Lavalley, J. C.; Elfallah, J.; Hilaire, L.; Lenormand, F.; Quemere, E.; Sauvion, G. N.; Touret, O. Reduction of CeO₂ by Hydrogen-Magnetic-Susceptibility and Fourier-Transform Infrared, Ultraviolet and X-Ray Photoelectron Spectroscopy Measurements. *J. Chem. Soc., Faraday Trans.* **1991**, *87* (10), 1601–1609.
- (3) Perrichon, V.; Laachir, A.; Bergeret, G.; Frety, R.; Tournayan, L.; Touret, O. Reduction of Cerias with Different Textures by Hydrogen and Their Reoxidation by Oxygen. *J. Chem. Soc., Faraday Trans.* **1994**, *90* (5), 773–781.
- (4) Trovarelli, A. Catalytic properties of ceria and CeO₂-containing materials. *Catal. Rev.-Sci. Eng.* **1996**, *38* (4), 439–520.
- (5) Diebold, U. The surface science of titanium dioxide. *Surf. Sci. Rep.* **2003**, *48* (5–8), 53–229.
- (6) Zhang, C. J.; Lindan, P. J. D. Multilayer water adsorption on rutile TiO₂(110): A first-principles study. *J. Chem. Phys.* **2003**, *118* (10), 4620–4630.
- (7) Lauritsen, J.; Foster, A.; Oleson, G.; Christensen, M.; Kuhnle, A.; Rostrup-Nielsen, J.; Clausen, B.; Reichling, M.; Besenbacher, F. Chemical identification of point defects and adsorbates on a metal oxide surface by atomic force microscopy. *Nanotechnology* **2006**, *17*, 3436–3441.
- (8) Lindan, P. J. D.; Zhang, C. J. Exothermic water dissociation on the rutile TiO₂(110) surface. *Phys. Rev. B* **2005**, *72* (7), 075439.
- (9) Lindan, P. J. D.; Zhang, C. J. Comment on “Molecular chemisorption as the theoretically preferred pathway for water adsorption on ideal rutile TiO₂(110)”. *Phys. Rev. Lett.* **2005**, *95* (2), 029601.
- (10) Zhang, C. J.; Lindan, P. J. D. Multilayer water adsorption on rutile TiO₂(110): A first-principles study. *J. Chem. Phys.* **2003**, *118* (10), 4620–4630.
- (11) Esch, F.; Fabris, S.; Zhou, L.; Montini, T.; Africh, C.; Fornasiero, P.; Comelli, G.; Rosei, R. Electron localization determines defect formation on ceria substrates. *Science* **2005**, *309* (5735), 752–755.
- (12) Fabris, S.; Vicario, G.; Balducci, G.; de Gironcoli, S.; Baroni, S. Electronic and atomistic structures of clean and reduced ceria surfaces. *J. Phys. Chem. B* **2005**, *109* (48), 22860–22867.
- (13) Nolan, M.; Parker, S. C.; Watson, G. W. CeO₂ catalysed conversion of CO, NO₂ and NO from first principles energetics. *Phys. Chem. Chem. Phys.* **2006**, *8* (2), 216–218.
- (14) Dudarev, S. L.; Botton, G. A.; Savrasov, S. Y.; Szotek, Z.; Temmerman, W. M.; Sutton, A. P. Electronic structure and elastic properties of strongly correlated metal oxides from first principles: LSDA+U, SIC-LSDA and EELS study of UO₂ and NiO. *Phys. Status Solidi A: Appl. Res.* **1998**, *166* (1), 429–443.
- (15) Kresse, G.; Furthmüller, J. Efficient iterative schemes for ab initio total-energy calculations using a plane-wave basis set. *Phys. Rev. B* **1996**, *54* (16), 11169–11186.
- (16) Perdew, J. P.; Burke, K.; Wang, Y. Generalized gradient approximation for the exchange-correlation hole of a many-electron system. *Phys. Rev. B* **1996**, *54* (23), 16533–16539.
- (17) Perdew, J. P.; Chevary, J. A.; Vosko, S. H.; Jackson, K. A.; Pederson, M. R.; Singh, D. J.; Fiolhais, C. Atoms, Molecules, Solids, and Surfaces—Applications of the Generalized Gradient Approximation for Exchange and Correlation. *Phys. Rev. B* **1992**, *46* (11), 6671–6687.
- (18) Perdew, J. P.; Wang, Y. Accurate and Simple Analytic Representation of the Electron-Gas Correlation Energy. *Phys. Rev. B* **1992**, *45* (23), 13244–13249.
- (19) Fabris, S.; de Gironcoli, S.; Baroni, S.; Vicario, G.; Balducci, G. Taming multiple valency with density functionals: A case study of defective ceria. *Phys. Rev. B* **2005**, *71* (4), 041102(R).
- (20) Mullins, D. R.; Radulovic, P. V.; Overbury, S. H. Ordered cerium oxide thin films grown on Ru(0001) and Ni(111). *Surf. Sci.* **1999**, *429* (1–3), 186–198.
- (21) Fabris, S.; de Gironcoli, S.; Baroni, S.; Vicario, G.; Balducci, G. Reply to “Comment on ‘Taming multiple valency with density functionals: A case study of defective ceria’”. *Phys. Rev. B* **2005**, *72* (23), 237102.
- (22) Blochl, P. E. Projector Augmented-Wave Method. *Phys. Rev. B* **1994**, *50* (24), 17953–17979.
- (23) Fontaine-Vive, F.; Johnson, M. R.; Kearley, G. J.; Howard, J. A. K.; Parker, S. F. How phonons govern the behavior of short, strong hydrogen bonds in urea–phosphoric acid. *J. Am. Chem. Soc.* **2006**, *128* (9), 2963–2969.
- (24) Henderson, M. A.; Perkins, C. L.; Engelhard, M. H.; Thevuthasan, S.; Peden, C. H. F. Redox properties of water on the oxidized and reduced surfaces of CeO₂(111). *Surf. Sci.* **2003**, *526* (1–2), 1–18.
- (25) Daturi, M.; Finocchio, E.; Binet, C.; Lavalley, J. C.; Fally, F.; Perrichon, V. Study of bulk and surface reduction by hydrogen of Ce_xZr_{1-x}O₂ mixed oxides followed by FTIR spectroscopy and magnetic balance. *J. Phys. Chem. B* **1999**, *103* (23), 4884–4891.
- (26) Tilocca, A.; Selloni, A. Structure and reactivity of water layers on defect-free and defective anatase TiO₂(101) surfaces. *J. Phys. Chem. B* **2004**, *108* (15), 4743–4751.
- (27) Kumar, S.; Schelling, P. K. Density functional theory study of water adsorption at reduced and stoichiometric ceria (111) surfaces. *J. Chem. Phys.* **2006**, *125* (20), 204704.
- (28) Finocchi, F.; Goniakowski, J. Interaction of a water molecule with the oxygen vacancy on the MgO(100) surface. *Phys. Rev. B* **2001**, *64* (12), 125426.